IgG Fab glycans hinder FcRn-mediated placental transport

Volkov, M.; Brinkhaus, M.; Schie, K.A. van; Bondt, A.; Kissel, T.; Kooi, E.J. van der; ... ; Woude, D. van der

IgG Fab Glycans Hinder FcRn-Mediated Placental Transport

Mikhail Volkov,*[,1] Maximilian Brinkhaus,[†,1] Karin A. van Schie,* Albert Bondt,[‡] Theresa Kissel,* Elvera J. van der Kooi,[†] Arthur E. H. Bentlage,[†] Carolien A. M. Koeleman,[‡] Steven W. de Taeye,[†] Ninotska I. Derksen,[§] Radboud J. E. M. Dolhain,[¶] Ute Braig-Scherer,[‖] Tom W. J. Huizinga,* Manfred Wuhrer,[‡] René E. M. Toes,* Gestur Vidarsson,[†] and Diane van der Woude*

Abs can be glycosylated in both their Fc and Fab regions with marked effects on Ab function and binding. High levels of IgG Fab glycosylation are associated with malignant and autoimmune conditions, exemplified by rheumatoid arthritis and highly Fab-glycosylated (~90%) anti-citrullinated protein Abs (ACPAs). Important properties of IgG, such as long half-life and placental transport, are facilitated by the human neonatal Fc receptor (hFcRn). Although it is known that glycosylation of Abs can affect binding to Fc receptors, little is known on the impact of IgG Fab glycosylation on hFcRn binding and transplacental transport. Therefore, we analyzed the interaction between hFcRn and IgG with and without Fab glycans in vitro with various methods as well as in vivo by studying placental transfer of Fab-glycosylated Abs from mothers to newborns. No effect of Fab glycosylation on IgG binding to hFcRn was found by surface plasmon resonance and hFcRn affinity chromatography. In contrast, studies in a cell membrane context revealed that Fab glycans negatively impacted IgG–hFcRn interaction. In line with this, we found that Fab-glycosylated IgGs were transported ~20% less efficiently across the placenta. This appeared to be a general phenomenon, observed for ACPAs, non-ACPAs, as well as total IgG in rheumatoid arthritis patients and healthy controls. Our results suggest that, in a cellular context, Fab glycans inhibit IgG–hFcRn interaction and thus negatively affect the transplacental transfer of IgG. As Fab-glycosylated Abs are frequently associated with autoimmune and malignant disorders and may be potentially harmful, this might encompass a regulatory mechanism, limiting the half-life and transport of such Abs. ***The Journal of Immunology*****, 2023, 210: 158–167.**

Immunoglobulin G represents the most abundant class of Igs in humans. Among its two main parts, the variable (Fab) domain is considered responsible for IgG binding specificity, whereas the constant (Fc) domain is thought to determine IgG effector functions and other properties, such as its half-life and transport. These latter effects are mainly facilitated via complement and various Fc receptors (1).

Among IgG Fc receptors, the human neonatal Fc receptor (hFcRn), expressed mostly intracellularly, plays a unique role in facilitating IgG homeostasis and transport. Circulating IgG is routinely taken up through pinocytosis by various cell types of hematopoietic origin as well as endothelial and epithelial cells. In the context of the decreasing pH in the developing endosomes, hFcRn binds IgG and rescues it from lysosomal degradation by mediating its transport back to the cell surface where it is released back into the circulation (2). In this manner, hFcRn brings about the relatively long half-life of IgG molecules of ~3 wk compared with 1 wk of similar-sized proteins such as IgA (3). Furthermore, high expression of hFcRn in syncytiotrophoblasts is responsible for placental transcytosis of IgG from mother to fetus during pregnancy, assuring immunological protection of the child in the first months after birth (4). In a similar manner, but with functionally different consequences, hFcRn expression at other epithelial sites has been found to mediate IgG transport in intestines, kidney, and liver (5, 6).

In the last few years, *N*-linked glycosylation of IgG has emerged as an important factor defining IgG properties and functions. *N*-linked glycosylation is a posttranslational modification by which oligosaccharides are attached to an asparagine within a consensus sequence, also known as an *N*-linked glycosylation site (N-X-S/T; where X is any amino acid except proline). In IgG Fc domains, *N*-linked glycosylation is highly conserved and it is restricted to one *N*-linked glycan

*Department of Rheumatology, Leiden University Medical Center, Leiden, the Netherlands; [†]Department of Experimental Immunohematology, Sanquin Research and Landsteiner Laboratory, Amsterdam UMC, University of Amsterdam, Amsterdam, the Netherlands; [‡]Center for Proteomics and Metabolomics, Leiden University Medical Center, Leiden, the Netherlands; [§]Department of Immunopathology, Sanquin Research and Landsteiner Laboratory, Amsterdam UMC, University of Amsterdam, Amsterdam, the Netherlands; [¶]Department of Rheumatology, Erasmus University Medical Center, Rotterdam, the Netherlands; and [‖]International Health Centre–Polikliniek Prins Willem, The Hague, the Netherlands

[1]M.V. and M.B. contributed equally to this work.

ORCIDs: 0000-0001-7577-2994 (M.V.); 0000-0002-7426-9980 (M.B.); 0000-0002-9703-2441 (K.A.v.S.); 0000-0002-0985-7903 (A.B.); 0000-0002-5749-8087 (T.K.); 0000-0002-7924-554X (A.E.H.B.); 0000-0002-7402-6380 (C.A.M.K.); 0000-0001-7915-9230 (S.W.d.T); 0000-0002-0189-2675 (N.I.D.); 0000-0002-0814-4995 (M.W.); 0000-0002-9618-6414 (R.E.M.T.); 0000-0001-5621-003X (G.V.).

Received for publication June 23, 2022. Accepted for publication November 8, 2022.

This work was supported by the ReumaNederland Project LLP5), as well as by the Innovative Medicines Initiative (IMI)–funded projects RTCure 777357 and Target-to-B LSHM18055-SGF (to R.E.M.T.). The work of M.B. and E.J.d.v.K. was funded by argenx. The PreCARA study was supported by UCB where UCB provided financial support; moreover, the PreCARA study was supported by the Dutch Arthritis Foundation (ReumaNederland Project LLP26).

M.V., M.B., K.A.v.S., A.B., R.E.M.T., G.V., and D.v.d.W. designed the research; M.V., M.B., K.A.v.S., A.B., T.K., E.J.v.d.K., A.E.H.B., and S.W.d.T. designed the experiments; R.J.E.M.D., U.B.-S., G.V., and D.v.d.W. organized the inclusion of participants and collection of samples; M.V., M.B., K.A.v.S., A.B., T.K., E.J.v.d.K., A.E.H.B., C.A.M.K., and N.I.D. performed the experiments; M.V., M.B., K.A.v.S., A.B., T.K., E.J.v.d.K., A.E.H.B., C.A.M.K., N.I.D., T.W.J.H., M.W., R.E.M.T., G.V., and D.v.d.W. participated in the analysis and interpretation of the data; and M.V., M.B., K.A.v.S., G.V., and D.v.d.W. wrote the manuscript. All authors contributed to and approved the manuscript.

Address correspondence and reprint requests to Dr. Diane van der Woude, Department of Rheumatology C1-R, Leiden University Medical Center, Albinusdreef 2, PO Box 9600, 2300 RC Leiden, the Netherlands. E-mail address: dvanderwoude@lumc.nl.

The online version of this article contains supplemental material.

Abbreviations used in this article: ACPA, anti-citrullinated protein Ab; FG, Fab-glycosylated; GE, glycoengineering; HEK, human embryonic kidney; hFcRn, human neonatal fc receptor; IVIg, i.v. IgG; LC, liquid chromatography; MS, mass spectrometry; NFG, non–Fab-glycosylated; QC, quality control; RA, rheumatoid arthritis; SNA, *Sambucus nigra* lectin; SPR, surface plasmon resonance; UHPLC, ultra-HPLC.

site at position N297 of each IgG H chain. The composition of Fc glycans is known to influence the interaction of IgG with FcγRs (7).

In Fab domains, *N*-linked glycosylation varies and is estimated to be present on ∼17% of IgG molecules (8, 9). Fab glycosylation is enriched on Abs with particular specificities, including anti-citrullinated protein Abs (ACPAs), anti-hinge region Abs, and anti-HIV-1 Abs (Refs. 9, 10, and M. N. Melo-Braga, M. B. Carvalho, M. C. E. Ferreira, and L. F. Felicori, manuscript posted on bioRxiv, DOI: 10.1101/2021.04.11.439351). In particular, ACPAs, the hallmarking autoantibodies in patients with rheumatoid arthritis (RA), exhibit very abundant *N*-linked Fab glycosylation, reaching ∼90% (9). This could be driven by chronic Ag exposure, which is known to introduce *N*-linked glycosylation motifs (11).

The influence of IgG *N*-linked glycosylation on transplacental transport has been actively investigated, although initially without distinguishing between Fc and Fab glycans. Some of these studies provided data suggesting increased transport of galactosylated IgG (12–14). Later studies, focusing on the Fc glycan composition, generally found no impact of the Fc glycan composition on transplacental transport (15, 16), except for one study reporting increased total IgG (of all IgG subclasses) Fc galactosylation in cord blood (17). As IgG1 generally shows higher galactosylation than IgG2, this discrepancy could potentially be explained by selective IgG1 transfer (15). Of note, the hFcRn binding site of IgG is distinct and distant from the FcγR binding site and consequently appears not to have the same crucial dependence on the highly conserved *N*-linked glycosylation of the Fc region (7, 18, 19), as FcγRs.

Fab glycans have been hypothesized to affect the structural and therapeutic properties of IgG-based medicines (11, 20). Recent studies on therapeutic Abs revealed that the exact composition and charge of the IgG Fab region can affect the half-life of IgG, suggesting that the interaction of IgG and hFcRn is more complex than anticipated (21–24). This finding also has possible implications for both hFcRn-mediated recycling and transcellular transport of Fab-glycosylated IgG. Thus, investigating the effect of Fab glycans on hFcRn binding will be an important step toward understanding the hFcRn biology and the functional properties of IgG Fab glycans.

In this study, we investigated whether Fab glycans influence IgG–hFcRn interaction using highly Fab-glycosylated ACPA IgG as model Abs. We employed several in vitro assays, including conventional surface plasmon resonance (SPR) and hFcRn affinity chromatography, as well as a novel cell-based competitive binding assay. The relevance of the in vitro observations was subsequently investigated in vivo by measuring IgG Fab glycosylation abundance in serum of women at delivery and in that of their newborns. In this manner, we aimed to comprehensively elucidate whether Fab glycans, by affecting the interaction with hFcRn, may influence IgG half-life and maternal–fetal transport.

Materials and Methods

Monoclonal IgG production, glycoengineering, and purification

ACPA IgG BCR sequences were isolated from citrulline-reactive human B cells of patients with RA, after which the recombinant mAbs were produced in a transitionary Freestyle 293-F cell (Life Technologies) transfection system and purified, all as described (25). Non–Fab-glycosylated (NFG) variants were produced by mutating the *N*-glycosylation sites in Fabs back to the respective germline sequence. All produced IgGs were of the IgG1 subclass. Addition of D-galactose substrate (Sigma-Aldrich) to the culture and coexpression with 1% β-1,4-*N*-acetylglucosaminyltransferase III (GnTIII), 2.5% α2,6-sialyltransferase 1 (ST6galT), and 1% β-1,4-galactosyltransferase 1 (B4GalT1) were used for glycoengineering (GE) (26).

Isolation of Fab-glycosylated IgG by Sambucus nigra *agglutinin lectin fractionation*

Intravenous IgG (IVIg) (Sanquin) enriched or depleted for Fab-sialylated IgG was obtained as described previously (27).

HPLC–size-exclusion chromatography

All Abs and Ab fragments as well as hFcRn were checked for aggregation in analytical HPLC–size-exclusion chromatography, as described previously (28).

Determining glycosylation profile of the produced mAbs

The glycosylation profile of the mAbs was analyzed by MALDI-TOF–mass spectrometry (MS), essentially as described before (29). In short, 10 μg of Ab was captured using CaptureSelect FcXL beads (Thermo Scientific), eluted with formic acid, dried, and denatured, and glycans were released with PNGase F. To stabilize the sialic acids, glycans were ethyl esterified by adding EDC/HOBt as described (29), with the exception that glycans were subsequently amidated by adding 25% ammonia solution (5:1 v/v derivatization solution/ammonia solution) followed by a 1-h incubation at 37°C. Glycans were purified using hydrophilic interaction liquid chromatography (LC)–solid phase extraction and spotted on an AnchorChip 800/384 as described. MALDI-TOF spectra were acquired using a rapifleX instrument (Bruker) in positive reflector ion mode using a *m/z* range of 900–4500, and 30,000 laser shots were accumulated at 5000 Hz. Spectra were smoothed and background subtracted using FlexAnalysis (Bruker). MassyTools was used to calibrate and integrate the spectra (30). Analytes were only retained when they fulfilled all of the following quality control (QC) criteria: 1) mass error between −25 and 25 ppm, 2) deviation from theoretical isotopic pattern (isotopic pattern quality) <25%, 3) signal-to-noise ratio >9. Per sample, the signal intensity of each glycan that passed the QC was normalized to 100%. To correct for monosialylation, the percentage sialylation of each sample was calculated using the following equation: (0.5 × summed percentage monosialylated glycans) + (1 × summed percentage disialylated glycans).

hFcRn affinity chromatography

hFcRn was produced and purified as described previously (28). Part of it was subsequently BirA-specifically biotinylated using BirA biotinylation kit (Avidity) according to the manufacturer's protocol. Three micrograms of biotinylated hFcRn was coupled to streptavidin-Sepharose (GE HealthCare) and packed in a 1-ml Tricorn 5/50 column (GE HealthCare), as described elsewhere (31).

Chromatography runs were performed on an ÄKTA Prime (GE HealthCare). Fifty to 100 μg of the IgG molecules was diluted in low-pH MES buffer (20 mM MES [Sigma-Aldrich], 150 mM NaCl [Sigma-Aldrich], pH 5.5). Following the equilibration of the column with the low-pH MES buffer, the samples were injected and a pH gradient was applied by an increasing concentration of the high-pH elution buffer (20 mM Tris-HCl [Thermo Scientific], 150 mM NaCl [Sigma-Aldrich], pH 8.8). The maximum peaks of the UV280 signals were used to determine retention times of the molecules.

SPR imaging

SPR measurements were performed on an IBIS MX96 device (IBIS Technologies), as described previously (32, 33). For measurement of hFcRn as a ligand, biotinylated hFcRn was spotted in 3-fold dilutions, ranging from 30 to 1 nM, and every spotting concentration was applied six times. Abs were then injected over the sensor in 2-fold dilution series starting at 0.24 nM until 500 nM. Regeneration after every sample was carried out with two injections of PBS + 0.075% Tween 80 (pH 8.7).

For measurement of hFcRn as an analyte, the Abs were randomly amine coupled onto a SensEye G Easy2Spot (Ssens, 1-09-04-006). The Abs were spotted in 2-fold dilutions, ranging from 30 to 7.5 nM in 10 mM acetate buffer (pH 4.5). After spotting, the sensor was deactivated with 100 mM ethanolamine (pH 8.5). hFcRn was then injected over the sensor in a 2-fold dilution series starting at 0.49 nM up to 1000 nM in PBS + 0.075% Tween 80 (pH 6 or 7.4). Regeneration was carried out after every sample by first injecting 20 mM Tris-HCl + 150 mM NaCl (pH 8.8) and then by injecting 20 mM H_3PO_4 (pH 2.3).

Calculation of the K_D was performed by equilibrium fitting to an interpolated R_{max} (maximal response) of 1000 resonance units for the Abs as analyte and R_{max} of 500 resonance units for the hFcRn as analyte (Supplemental Fig. 1).

hFcRn-expressing cells

Human embryonic kidney (HEK) cells, stably expressing hFcRn marked with GFP (HEK-hFcRn-GFP cells), were cultured in RPMI 1640 (Thermo Scientific) containing 10% (v/v) FCS, 4 mM L-glutamine (Thermo Scientific), 100 U/ml penicillin, and 100 μg/ml streptomycin (Thermo Scientific) in Nunclon Delta surface 80-cm^2 flasks (Thermo Scientific). When cells were 80–90% confluent, cells were passaged with 0.05% (m/v [mass per volume]) trypsin with 0.02% (m/v) EDTA (Thermo Scientific).

hFcRn surface competitive binding assay

HEK-hFcRn-GFP cells were harvested as described above and the assay was performed as described previously (34). The assay was performed on ice at 4°C to prevent physiological uptake. In brief, cells were washed with PBS containing 1% (v/v) FCS and 20 mM MES (Sigma-Aldrich) at pH 6.0. Premixes containing IgG glycovariants or IgG1-Fc only with DyLight 650–labeled (Thermo Scientific) anti-hFcRn Fab (35) in the same buffer were prepared and coincubated with 1×10^5 cells/per well for 30 min on ice in the dark. Cells were spun down at 450 × *g* at 4°C for 3 min, washed once with 150 µl of ice-cold PBS containing 1% FCS (v/v) and 20 mM MES, at pH 6.0, spun down as described above and washed with 150 µl of ice-cold PBS containing 1% (v/v) FCS at pH 7.4 before they were fixed using the BD Cytofix/Cytoperm fixation/permeabilization kit (BD Biosciences) according to the manufacturer's instructions. Cells were subsequently washed twice with 150 µl of ice-cold PBS containing 1% (v/v) FCS at pH 7.4, resuspended in 100 µl of the same buffer, and measured with flow cytometry. Flow cytometry measurements were performed using a BD FACSCanto II cell analyzer, BD LSR II, or BD LSRFortessa and analyzed using BD FACSDiva software (all from BD Biosciences). Data were analyzed using FlowJo 10.7.1 software (BD Biosciences). hFcRn surface expression on HEK-hFcRn-GFP cells and hFcRn binding of the anti-hFcRn Fab were confirmed separately, as described elsewhere (34). Geometric mean fluorescence intensity reflected how much of the Alexa Fluor (AF) 650–labeled anti-hFcRn Fab was outcompeted by the IgG glycovariants or IgG1-Fc only. Geometric mean fluorescence intensity values were normalized using medium only as 100% (no competition) and IgG1-Fc only as 0% (maximum observed competition). The resulting percentages were then subtracted from 100% to derive the resulting "hFcRn occupancy" value. This value indicated how well a molecule outcompetes binding of the anti-hFcRn Fab as compared with the medium control.

Patient samples

Two cohorts of mothers with ACPA-positive RA together with their newborns were included in this study: the OOIEVAAR study (six mothers and six newborns), from the Leiden University Medical Center, and the PreCARA study (six mothers and seven newborns, with one pair of twins), from the Erasmus University Medical Center. For mothers included in OOIEVAAR, blood was collected at delivery; for five out of six mothers included in PreCARA, blood was collected between 28 and 32 wk of pregnancy, and for one mother, blood was collected at 6 wk after delivery. For all newborns, cord blood samples were used. For healthy donors, plasma was collected from 38 healthy mothers and the umbilical cord of their newborns directly after delivery (average 37.8 wk) (14). Prior to each of the studies, participating mothers provided written informed consent. The collection of plasma samples and clinical data were in compliance with the Declaration of Helsinki and was approved by the Ethics Committee of the Leiden University Medical Center (P13.191 for OOIEVAAR and P02-200 for the study of healthy donors) and Erasmus MC (MEC-2011-032) for PreCARA (36). Furthermore, all experiments were performed in accordance with the relevant ethical guidelines and regulations.

Isolation of ACPA IgG, non-ACPA IgG, and total IgG

For all samples of mothers with ACPA-positive RA and their newborns, ACPAs were isolated essentially as described before (37). In short, ACPAs were captured using cyclic citrullinated peptide 2 (CCP2)–coupled beads. The ACPA-containing eluates as well as the flowthrough of the CCP2 isolation (i.e., non-ACPAs) were subsequently loaded onto protein G beads (GE Healthcare) to isolate IgG, resulting in ACPA IgG and non-ACPA IgG, respectively. For the healthy donor samples, total IgG was isolated using IgG Fc (Hu) beads (Thermo Fisher Scientific) (29).

Determining percentage Fab glycosylation

For ACPA IgG and non-ACPA IgG, the degree of Fab glycosylation was determined by ultra-HPLC (UHPLC), as described before (37). In brief, glycans were released with PNGase F and labeled with 2-aminobenzoic acid and 2-picoline borane. Two–amino acid-labeled glycans were purified using hydrophilic interaction LC–solid phase extraction. Samples were analyzed using UHPLC, peaks were aligned and annotated using Chromeleon v7.2, and chromatograms were exported. Chromatograms were checked blindly, and samples were excluded in case of aberrant peak distribution and/or lacking the three most abundant Fc glycan peaks (H3N4F1, H4N4F1, and H5N4F1). In this structural coding, "H" stands for hexose (mannose or galactose), "N" stands for *N*-acetylglucosamine, "F" stands for fucose, and "S" stands for sialic acid. Data analysis was performed as described earlier (37). In brief, HappyTools (version 0.0.2, built 171124a) (38) was used to calibrate, baseline correct, and integrate the peaks. The degree of Fab glycosylation was calculated by dividing the summed area under the curve of the three most abundant Fab glycan peaks (H5N5F1S1, H5N4F1S2, and H5N5F1S2) by the summed area under the curve of the three most abundant Fc glycan peaks (H3N4F1, H4N4F1, and H5N4F1) (9). The glycoforms for the calculation were selected based on previous observations showing their exclusive presence on either the Fab domain or the Fc domain of ACPA IgG molecules (39, 40), which had been determined by analyzing glycans on Fab and Fc domains separately (9). As some common Fab glycans can be sometimes found on Fc, we analyzed Fc glycosylation separately to control for possible differences between mothers and children.

For total IgG from healthy donors, the degree of Fab glycosylation was calculated from the total IgG glycan profiles obtained by MALDI-TOF-MS. Glycan release, ethyl esterification, glycan purification, MALDI-TOF-MS, and data processing were performed as described elsewhere (29). The degree of Fab glycosylation was calculated by dividing the summed relative intensities of the three most abundant Fab glycan peaks (H5N5F1S1, *m/z* 2331.85; H5N4F1S2, *m/z* 2447.89; and H5N5F1S2, *m/z* 2650.97) by the summed relative intensities of the three most abundant Fc glycan peaks (H3N4F1, *m/z* 1485.53; H4N4F1, *m/z* 1647.59; and H5N4F1, *m/z* 1809.64) (9).

Fc glycosylation analysis

Ab Fc glycosylation was analyzed by MS essentially as described (41). In short, isolated ACPA IgG, non-ACPA IgG, or mAbs were captured using protein G beads (GE HealthCare), eluted, dried by vacuum centrifugation, and digested with trypsin that was treated with L-(tosylamido-2-phenyl)ethyl chloromethyl ketone (TPCK) (Sigma-Aldrich). The resulting glycopeptides were subsequently analyzed by nano-LC-MS using an ACQUITY UPLC BEH C18 column (130 Å, 1.7 µm; 75 µm × 100 mm; Waters) for the glycopeptide separation. Mass spectrometric signals of IgG1 glycopeptides (peptide sequence: EEQYNSTYR) and IgG2/3 glycopeptides (shared peptide sequence: EEQFNSTFR) were aligned, calibrated, and integrated using LaCyTools (version 1.1.0-α) (42). A glycopeptide was determined to be present when fulfilling the following QC criteria: 1) mass error between −10 and 10 ppm, 2) deviation from theoretical isotopic pattern (isotopic pattern quality) <20%, 3) signal-to-noise ratio >9.

For mAbs, per sample, the signal intensity of each glycan that passed the QC was normalized to 100%. Samples were then stratified on absence or presence of glycoengineering. Per group, all glycopeptides containing >5% of the signal intensity are shown in Supplemental Fig. 2.

For ACPA and non-ACPA IgG, a glycopeptide was included in the analysis in case it passed the QC in either >50% of the mothers or >50% of the newborns. The signal intensity of all included glycopeptides was normalized to 100% per sample. For each sample, the relative intensity levels of H3N4F1, H4N4F1, H5N4F1, H5N5F1S1, H5N4F1S2, and H5N5F1S2 are shown in Supplemental Fig. 3.

Data availability

The datasets generated during and/or analyzed during the current study are available from the corresponding author on reasonable request.

Results

Generation of mAbs with four different glycosylation patterns

To investigate the role of Fab glycans on the hFcRn–IgG interaction in a controlled manner, we generated recombinant mAbs with distinct glycosylation patterns. To this end, three ACPA IgG clones (7E4, 3F3, and 1F2) were selected (25), based on the presence of multiple *N*-linked glycosylation sites in the Fab region. To control for the specific impact of Fab glycans, four glycovariants were generated for each of the ACPA clones: Fab-glycosylated (FG) and NFG, each produced with and without GE (as described in *Materials and Methods*) (Fig. 1A). In particular, the variants either 1) harbored (only) Fc glycans with relatively low expression of galactose, sialic acid and bisecting GlcNAc (NFG); 2) (only) Fc glycans abundantly expressing galactose, sialic acid, and bisecting GlcNAc (NFG+GE); 3) Fc and Fab glycans with relatively low expression of galactose, sialic acid, and bisecting GlcNAc (FG); or 4) Fc and Fab glycans abundantly expressing galactose, sialic acid, and bisecting GlcNAc (FG+GE). The reason to glycoengineer the produced Abs is found in the rationale that Fab glycans, unlike Fc glycans, of human serum Abs (including ACPAs) are highly sialylated (9), a feature normally not present on mAbs produced by HEK cells. GE had a limited

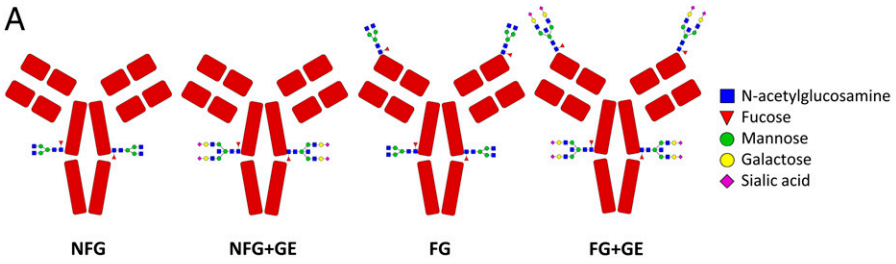

B

Clone	Isotype, light chain	Glyco-variant	Number and location of Fab-glycans	Theoretical pI: mAb + glycans (0% sialylation)	Theoretical pI: mAb + glycans (100% sialylation)	Observed mono-sialylation (%)	Observed bi-sialylation (%)
3F3	IgG1κ	NFG		6.49	6.24	0.2	0.0
		NFG+GE				18.0	2.6
		FG	2 * HC-FR3 1 * LC-FR3	6.49	5.68	17.6	3.5
		FG+GE				26.8	11.8
7E4	IgG1λ	NFG		8.34	7.66	0.0	0.0
		NFG+GE				21.8	1.0
		FG	1 * HC-CDR1 1 * LC-FR1	8.09	6.40	9.7	1.2
		FG+GE				31.2	16.1
1F2	IgG1λ	NFG		8.32	7.75	0.9	0.0
		NFG+GE				16.1	2.6
		FG	1 * HC-CDR1	8.32	6.45	22.7	3.9
		FG+GE	1 * HC-CDR2/FR3 1 * LC-FR1			33.8	7.8

FIGURE 1. Glycovariants of monoclonal IgG and their characteristics. (**A**) Schematic representation of the IgG glycovariants. (**B**) Characteristics of the clones and the glycovariants. The theoretical pI was calculated using Protein Tool from Prot pi, assuming disulfide bonds between all cysteines and glycans (Fc and Fab) having complex biantennary structures. The pI is given for the theoretical situation in which either 0% or 100% of glycans are sialylated. The observed percentage sialylation was derived from the combined analysis of Fc and Fab glycans, as determined by MALDI-TOF-MS. FG, Fab-glycosylated; GE, glycoengineering; NFG, non–Fab-glycosylated; pI, isoelectric point.

effect, but it increased the level of glycosylation and sialylation considerably (Fig. 1), bringing it closer to what is observed in human serum (43). Another limitation of GE was its influence on Fc glycosylation (Supplemental Fig. 2); hence, four glycovariants were required to investigate the specific effect of (sialylated) Fab glycans.

For all variants, the level of sialylation was determined by MALDI-TOF-MS (Fig. 1B), with the percentage sialylation being calculated per fully sialylated glycan, including all Fab and Fc glycans. Sialylation, stimulated by the added GE enzymes, appeared to affect mainly Fab glycans with a limited effect on Fc glycans (Fig. 1B, Supplemental Fig. 2). The integrity of all molecules was tested in HPLC–size-exclusion chromatography, confirming all IgG variants to be generally monomeric and the (expected) size shift for FG as compared with NFG was observed, indicative of the presence of Fab glycans (Supplemental Fig. 4). The generated ACPA monoclonal IgG variants, each having several differently located Fab glycans (Fig. 1B), were subsequently used to investigate the impact of Fab glycans on the IgG–hFcRn interaction.

No impact of Fab glycosylation on IgG–hFcRn interaction in SPR

To investigate the effect of these four different glycovariants on IgG–hFcRn interaction in vitro, we employed our SPR platform. Two different setups were used (Fig. 2, Supplemental Fig. 1) with immobilization of either hFcRn (setup 1) or IgG (setup 2) on the sensor (ligand) (Fig. 2A, 2C), as described elsewhere (44). In the setup in which hFcRn acted as the ligand, we observed a general trend for a higher apparent affinity of NFG Abs as compared with the FG variants, although the observed differences in apparent affinities did not exceed 1.5-fold (Fig. 2A, 2B). In the setup in which IgG acted as the ligand, the differences were even substantially smaller (Fig. 2C, 2D). Overall, SPR measurements did not show meaningful differences between the glycovariants, indicating that Fab glycans do not strongly affect the affinity of IgG binding to hFcRn.

No impact of Fab glycosylation on retention times in hFcRn affinity chromatography

As hFcRn affinity chromatography has been suggested to better predict in vivo clearance rates (21), we next measured retention times of the Ab variants in hFcRn affinity chromatography. Anti-trinitrophenyl IgG1 and its mutant bearing 3 aa substitutions in the IgG-Fc (I253A/H310A/H435A), known to abrogate IgG binding to hFcRn (45), were used as controls. As expected, nonmutated anti-trinitrophenyl IgG1 showed good retention, whereas the I253A/H310A/H435A mutant showed no hFcRn retention (Fig. 3A). The elution peaks of the ACPA glycovariants largely overlapped for 7E4 and 3F3 (Fig. 3B, 3C). For 1F2, however, FG+GE and even more so FG showed less retention than the NFG counterparts (Fig. 3D). Thus, also hFcRn affinity chromatography did not indicate a consistent effect of Fab glycans on hFcRn binding.

Fab glycans hinder binding to membrane-associated hFcRn

Next, we measured binding of the Ab glycovariants to membrane-associated hFcRn in our recently described hFcRn surface competition assay (Fig. 4A) (34). In this study, ACPA clones with FG bound membrane-associated hFcRn significantly worse than their NFG counterparts. The strength of this effect varied between clones (Fig. 4B–D). GE of these clones resulted in some differences between the variants in some of the clones (either NFG versus NFG+GE or FG+GE); however, these differences were not reproducible across difference clones, indicating that the charge of sialic acid–containing species incorporated by GE does not play a key role.

To investigate whether this is applicable to all IgGs (beyond ACPAs), we investigated this in polyclonal IgG from healthy donors. To study that, we used *Sambucus nigra* agglutinin (SNA) fractionation, as it was previously shown to efficiently isolate the Fab-glycosylated IgG fraction when applied to IgG from serum (11, 46), resulting in Fab glycan-enriched (SNA-positive) and Fab glycan-depleted (SNA-negative) IgG. In line with the results of the monoclonal ACPA IgG variants, we found the SNA-negative IVIg fraction (without sialic acid-containing Fab glycans) to bind significantly better to membrane-associated hFcRn, compared with the SNA-positive IVIg fraction (with these glycans) (Fig. 4E), indicating that Fab glycans generally hinder IgG binding to membrane-associated hFcRn.

In contrast to the results generated by SPR and affinity chromatography, these results indicate that Fab glycans negatively affect binding of IgG to hFcRn in vitro when tested with membrane-associated hFcRn.

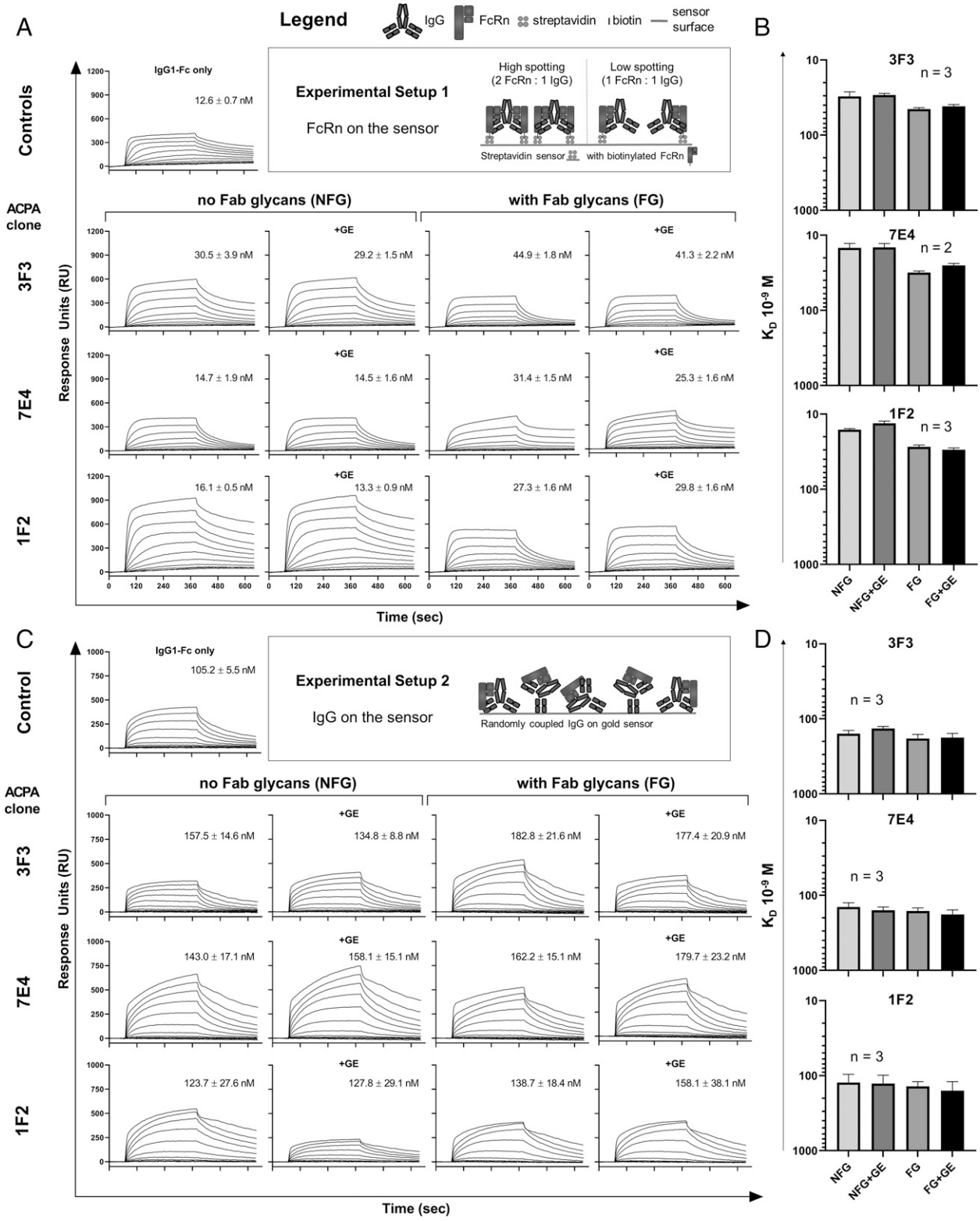

FIGURE 2. No differences between Fab glycovariants in binding to hFcRn at pH 6.0. (**A**) Sensorgrams of binding of IgG glycovariants and IgG1-Fc only to hFcRn as measured by SPR at pH 6.0 with FcRn as ligand (setup 1). Biotinylated hFcRn was immobilized on a streptavidin sensor, and IgG variants were titrated from 0.12 to 500 nM. The numbers indicate average K_D values of three independent experiments and the corresponding SD (in nM). K_D values were calculated by fitting a 1:1 Langmuir binding model. In order to fit this model, concentrations >125 nM were excluded for the calculations. Fits used to calculate apparent affinities reported in this figure can be found in Supplemental Fig. 3A. Traces shown here only show data used for affinity calculations. (**B**) K_D values of measurements at pH 6.0 as described above plotted as histograms. (**C**) Sensorgrams of binding of hFcRn to IgG glycovariants and IgG1-Fc only as measured by SPR at pH 6.0 with IgG (fragment) as ligand (setup 2). IgG variants were randomly coupled sensors, and soluble hFcRn was titrated from 0.49 to 500 or 1000 nM. K_D values were calculated as described above. No concentrations were excluded. Fits used to calculate apparent affinities reported in this figure can be found in Supplemental Fig. 3B. (**D**) K_D values of measurements at pH 6.0 as described above plotted as histograms. Data in (A) and (C) are representative of two or three independent SPR experiments, the results of which are summarized in (B) and (D), respectively. No statistical analysis was performed.

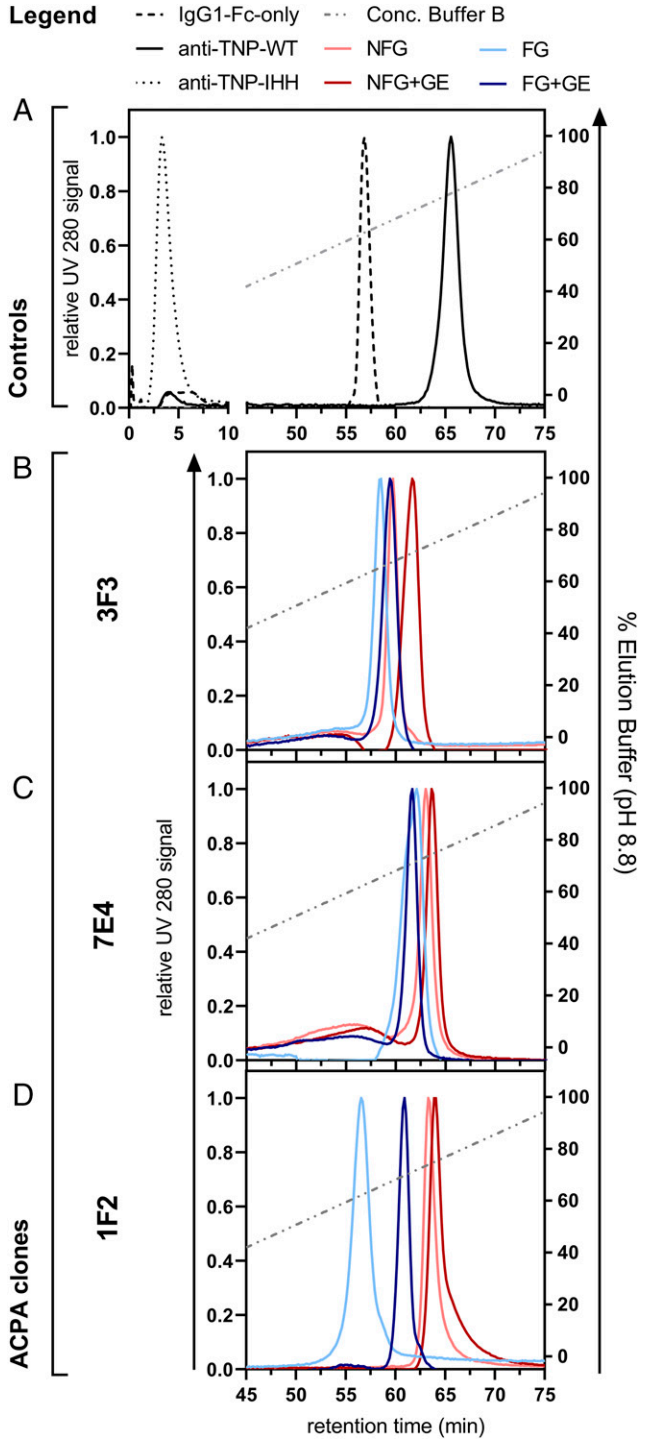

FIGURE 3. No clear differences in hFcRn affinity chromatography between IgG glycovariants. Chromatograms were obtained from comparing elution volume (pH-gradient elution from pH 5.5 to 8.8) on an hFcRn affinity column, presented as relative UV280 nm signal normalized to the maximum response. (**A**–**D**) Shown are one experiment of (A) controls and a representative of two experiments of the glycovariants of ACPA clones (B) 3F3, (C) 7E4, and (D) 1F2. No statistical analysis was performed. IHH, I253A/H310A/H435A; TNP, trinitrophenyl.

Fab glycans impair transplacental transfer of IgG from mothers to their newborns

We then wondered whether Fab glycan-containing IgG molecules are transferred less efficiently across the placenta, which is a hFcRn-dependent process. To investigate whether Fab glycans can indeed affect the hFcRn IgG transport in vivo, we compared abundance of Ab Fab glycosylation in mothers with RA and their newborns. We focused on mothers with RA, as the hallmarking autoantibodies in RA, ACPAs, express high levels of Fab glycans. To this end, ACPAs were isolated from maternal and cord blood resulting in an ACPA IgG and a non-ACPA IgG fraction. In these two fractions, as well as in total IgG from healthy mothers and their newborns, we analyzed the IgG glycosylation pattern using UHPLC and subsequently calculated the percentage of Fab glycosylation (Fig. 5A). Due to the limited volume of sample obtained, we could successfully isolate ACPAs of only six mother/child pairs.

As expected, the percentage of Fab glycosylation was very high for ACPA IgG (9). Strikingly, in all six pairs, abundance of ACPA Fab glycosylation was ~20% lower in newborns than in their mothers (Fig. 5B). These measurements were complemented by the ACPA-negative IgG fraction, in which, despite substantially lower levels of Fab glycosylation, a similar 20% difference between mothers and newborns was observed (Fig. 5C).

To further validate these findings, differences in Fab glycosylation abundance were analyzed in a separate cohort of 38 healthy mother/child pairs, where IgG-released glycans were measured with a different technique, that is, MALDI-TOF-MS (Fig. 5D). In line with the observations in RA mothers and their newborns, total IgG of the newborns from healthy mothers contained less Fab-glycosylated glycans in comparison with the maternal blood. These findings are thus in line with the observations from the hFcRn binding assay and indicate that Fab glycans impair IgG–hFcRn interaction.

Separate analysis of Fc glycosylation indirectly confirmed decreased Fab glycosylation in newborns

Because the formula used to calculate the approximate percentage of Fab glycosylation is based on the three known predominant Fc glycans in adults, we wanted to confirm that the same Fc glycans are the predominant ones in newborns. Therefore, Fc glycopeptides of IgG1, IgG2, and IgG3—together making up 96% of total IgG—of mothers and newborns were analyzed using LC-MS (47). The IgG Fc glycosylation pattern was found to be largely similar between mothers and their newborns, and only minor differences were observed in the three Fc glycans used for calculating the percentage of Fab glycosylation (Supplemental Fig. 3). In addition, the abundance of the three known Fab-specific glycans was very low when measured in the Fc fraction, showing that these glycans are, as expected, genuine Fab glycans in both mothers and newborns.

Discussion

In this study, we observed that the presence of Fab glycans on IgG diminishes IgG–hFcRn interaction. This observation was made using a cell-based assay, whereas no clear indications of this effect were noted by "conventional" biochemical assays that lack the cellular context. Importantly, the negative effect of IgG Fab glycans on hFcRn binding was confirmed by in vivo data, as a comparison of IgG Fab glycosylation in paired sera of mothers and their newborns showed a lower level of Fab glycosylation of IgG in the newborns, which was evident in both RA patients and healthy individuals, controlled by a separate Fc glycan analysis. As the presence of IgG in newborns relies solely on transcytosis by hFcRn, these data are in line with the observation that Fab glycosylation inhibits the binding of human IgG to hFcRn (16, 48, 49).

Our study indicates that a membrane context plays an important role in hFcRn biology, as the data collected with conventional non-cellular in vitro assays, being SPR and affinity chromatography, differed from the data collected using a cellular competition binding assay. Differences observed in Fig. 4 between FG and NG clones

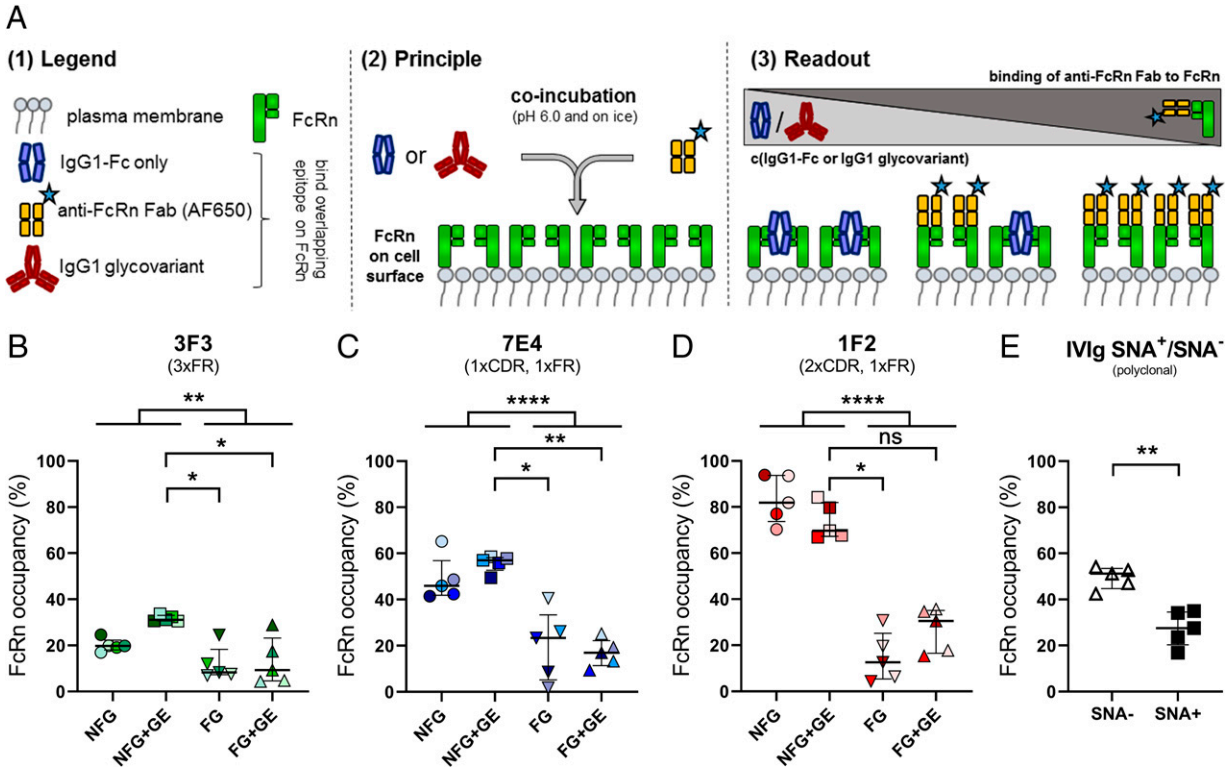

FIGURE 4. Fab glycosylation hinders IgG binding to membrane-associated hFcRn. (**A**) Illustration of the principle of the hFcRn surface competition assay. The IgG glycovariants or IgG1-Fc only are coincubated at a fixed concentration with an Alexa Fluor 650–labeled anti-hFcRn Fab on ice on hFcRn-overexpressing HEK cells and measured by flow cytometry. The signal measured for IgG1-Fc only is defined as 100% hFcRn occupancy, medium control as 0% hFcRn occupancy. (**B**–**E**) Fab glycosylation hinders binding of IgG variants (FG) to membrane-associated hFcRn compared with non–Fab-glycosylated variants (NFG) for the assayed ACPA clones (B) 3F3, (C) 7E4, and (D), 1F2 as well as for (E) Fab sialylation-enriched IVIg fractions (IVIg SNA^+), compared with Fab sialylation-depleted IVIg. Data of five independent experiments are shown. Statistical analysis was performed using a Mann–Whitney test (pooled NFG versus FG) or Kruskal–Wallis test (single comparisons). $*p < 0.05$, $**p < 0.01$, $****p < 0.0001$.

could potentially be explained by competitive binding of Siglecs on the cell surface to the sialic acids located on Fab glycans. This, however, appears unlikely, as HEK cells lack Siglec expression (50) and no evident trend was observed between the differentially sialylated FG and FG+GE variants across the clones (Fig. 4).

Regarding the differences between the observations performed with different methods, a similar apparent discrepancy between IgG-hFcRn SPR measurements and results that depended on a cellular context has been noted before, in studies investigating clearance rates in hFcRn transgenic mice (21, 51). Conversely, affinity chromatography has been shown to correlate closer with the in vivo data for certain sets of Abs (21). Nevertheless, this technique exclusively relies on direct biochemical protein–protein interaction and does not reflect the membrane context. Our data presented suggest that the use of cell-based assays is likely of relevance to come to a full understanding of IgG–hFcRn interactions.

The inhibitory effect of the Fab glycans on the IgG–hFcRn interaction could potentially be explained by (one of) three different mechanisms: charge-based interactions due to negatively charged sialic acids located on Fab glycans, steric hindrance resulting from the bulkiness of Fab glycans, and disruptive interaction with the Fab domain regions participating in IgG–hFcRn binding. Interestingly, it has been previously shown that charge distribution on the Fab domain can influence the IgG–hFcRn interaction (21, 23, 52). However, the negative charge of the Fab glycans located on GE ACPA IgGs did not appear to have a clear effect on the IgG–hFcRn interaction in the cellular assay experiments.

Evidently, it was not the structure, but the presence/absence of the Fab glycans that determined the difference in the IgG–hFcRn binding. This is in line with recent findings that the presence or absence of Fab domains affects the binding of IgG to hFcRn (24, 34). It is likely that the exact location of a Fab glycan determines its ability to interfere with the IgG–hFcRn interaction, as the extent of the diminishing effect did not simply correlate with the number of Fab glycans on an IgG clone, as measured by the cellular study. Glycans expressed by CDRs (53), regions involved in Ag binding, are likely to be highly exposed and thus have a higher chance of contributing to Fab-mediated effects. This is in line with our observations of 7E4 and 1F2 (with Fab glycans located at CDRs) showing higher differences between FG and NFG variants as compared with 3F3 (with Fab glycans located exclusively at framework regions outside of CDRs). A previous study hinted at the impact of specifically positioned Fab glycans (within CDRs) on IgG-hFcRn affecting IgG half-life in BALB/c mice (54). Another study in hFcRn transgenic mice suggested a stronger impact of CDR-located alterations in Fab domain sequences as compared with alterations in the framework region (23). Moreover, crystallization studies of ACPAs have shown that ACPA Fab glycans are positioned in close vicinity to the Ag-binding pockets and likely form hydrogen bonds with CDR structures (26); it was also shown that the back mutation of the *N*-glycosylation site back to the germline does not affect the structure of the Fab, thus suggesting that the only difference between FG and NFG variants is the presence or absence of Fab glycans. Overall, our results suggest that Fab glycans can directly interfere with IgG–hFcRn interaction and the Fab glycan location is important; however, it is not possible to conclude whether it is the steric hindrance or possible biochemical interaction (e.g., via hydrogen bonds) with the CDRs that explains the observed effect.

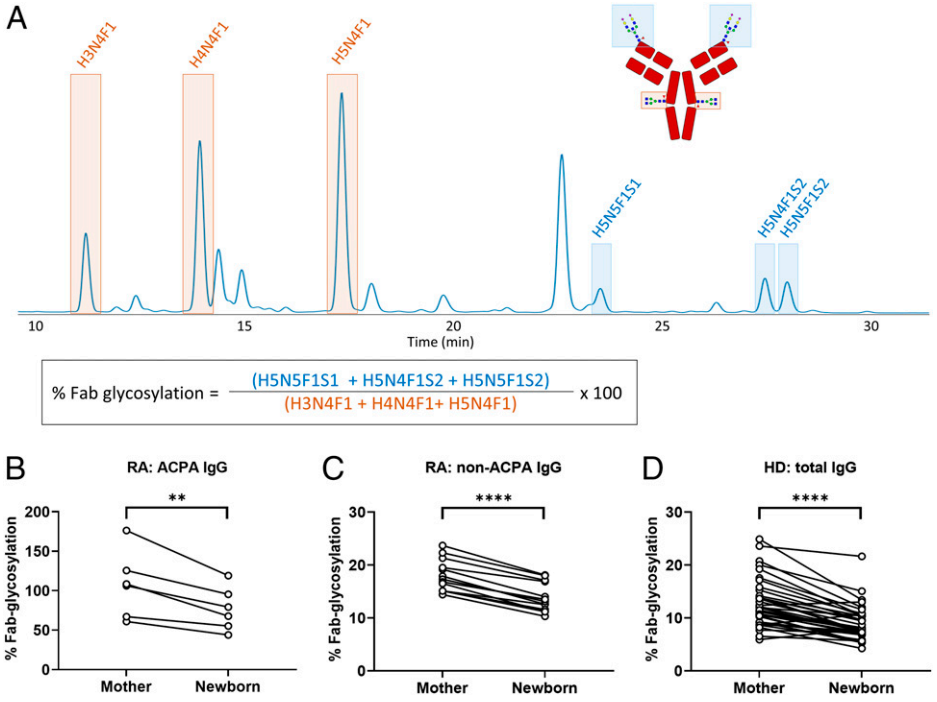

FIGURE 5. Fab glycosylation is decreased in newborns as compared with their mothers. (**A**) Example HPLC chromatogram of IgG glycans, and the calculation of the percentage Fab glycosylation. Fc glycans used for calculation are marked with orange frames, Fab glycans used for calculation are marked with blue frames. HappyTools was used to determine area under the curve and calculate relative abundances of the respective glycans. (**B**) Percentage Fab glycosylation in ACPA IgG from mothers with RA and their newborns. (**C**) Percentage Fab glycosylation in non-ACPA IgG from mothers with RA and their newborns. (**D**) Degree of Fab glycosylation in total IgG from healthy mothers (HD) and their newborns. F, fucose; H, hexose (mannose or galactose); N, *N*-acetylglucosamine; S, sialic acid. Statistical analysis was performed using a *t* test after normality testing (mother versus newborn). $^{**}p < 0.01$, $^{****}p < 0.0001$.

Another potential mechanism, potentially contributing to the differences observed in Fig. 4, can be competition of surface lectins with hFcRn for binding Fab-glycosylated Abs; lectin knockouts could potentially be implemented to test for it. Nevertheless, recently published data with the same method showed that the presence of Fab regions itself (without Fab glycans) impairs the internalization pathway of FcRn upon IgG engagement (34). These data indirectly contribute to the potential Fab-mediated bulk effect, enhanced by the presence of Fab glycans.

The role of Fab glycosylation in Ab biology is poorly understood. While a relatively low percentage of the IgG pool carries Fab glycans in healthy individuals (~17%), Fab glycosylation has been shown to be more abundant in autoimmune diseases, such as RA (9), Sjögren's disease (55), anti-neutrophil cytoplasmic Ab–associated vasculitis (56) and others. The underlying mechanisms remain unclear; however, introduction of Fab glycosylation sites was suggested to serve as a mechanism to escape critical immune checkpoints and play a role in the breach of tolerance toward self-antigens (26). Additionally, particularly high Fab glycosylation abundance was observed in the context of malignancies, such as B cell follicular lymphoma (57), multiple myeloma (58), and melanoma (59). In view of these observations, one could argue that Fab glycosylation appears to be associated with pathological conditions (i.e., autoimmunity, malignancy) and that impaired placental transfer and the shortened half-life of Fab-glycosylated IgG (resulting from hindered interaction with hFcRn) suggest the presence of an evolutionarily conserved protective mechanism.

Although, to our knowledge, our study provides novel insights into the role of IgG-associated *N*-linked glycans on hFcRn-mediated IgG homeostasis and transport, it also has several limitations. Although our data indicate that Fab glycans hamper the IgG–hFcRn interaction, structural and mechanistic studies are required to pinpoint the nature of the Fab glycan-mediated interference. The importance of the glycan composition (either Fab or Fc), that is, galactosylation/sialylation, may be to some extent underestimated, as our engineered variants were not 100% sialylated as often seen in vivo, a choice we made to generate enhanced sialylated Fab IgG without affecting the Fc glycosylation extensively. Additionally, the influence of the Fc glycosylation profile on IgG–hFcRn interaction is a debated topic (15–17, 51, 60–62), addressing which, however, was not the aim of this study. Moreover, the potential role of the exact Fab glycan position in the CDR or framework region was not investigated in great detail. In the in vivo part of the study, we could not measure the Fab glycosylation separately from Fc, as that necessitated additional processing of IgG, requiring an amount of sample that is difficult to obtain in the case of cord blood. Instead, we used an established method of Fab glycosylation abundance calculation (4, 38, 63), which, however, results in approximate Fab glycosylation abundances. Furthermore, we did not investigate a potential role of lectins competing with hFcRn for surface binding of Fab-glycosylated Abs; however, data presented in a recently published study employing the same method further confirm the bulk-effect hypothesis outlined in this paper by comparing IgGs with a different number of Fabs (34). Nevertheless, to our knowledge, this is the first study to focus specifically on the influence of Fab glycans on IgG–hFcRn interaction with a wide range of in vitro methods, which was complemented by the in vivo observations in humans. Importantly, the data obtained with our novel (to our knowledge), fast, and scalable cell-based assay fully aligned with the measurements performed in mother/child samples, thus confirming the robustness of our observations.

Potential future steps could include replication of these experiments with other Fab-glycosylated monoclonal IgGs, such as myeloma or lymphoma IgGs, Fab glycovariants with more contrasting differences in Fab galactosylation/sialylation profile, and thorough investigation of the mechanism responsible for this effect, including removing and adding *N*-glycosylation sites by targeted mutations and more elaborate approaches, investigating biochemical interaction between the Fab glycan and hFcRn in the membrane context. Furthermore, the exact role of surface lectins can be tested by using lectin knockout cells.

Overall, these data indicate that Fab glycans may play an important role in IgG homeostasis and transport by affecting the interaction between IgG and hFcRn. Although the precise mechanism is yet to be determined, Fab-glycosylated IgGs appear to interact less well with membrane-associated hFcRn, an effect that could possibly be influenced by the exact Fab glycan location within the Fab region.

Our study further illustrates the challenges related to investigation of hFcRn biology, as a wide range of various methods turned out to be necessary to identify a pattern in the effect of Fab glycans on IgG–hFcRn interaction. Our findings can further improve our understanding of the Ab biology and mechanisms regulating IgG homeostasis and transport.

Acknowledgments

We thank Dr. Theo Rispens for providing the SNA^+ and SNA^- IVIg fractions and for fruitful discussions, as well as Gerrie Stoeken-Rijsbergen, Nivine Levarht, and Astrid Brehler for help with IgG production.

Disclosures

The work of M.B. and E.J.v.d.K. was funded by argenx. G.V. serves as a consultant to argenx. The other authors have no financial conflicts of interest.

References

1. de Taeye, S. W., T. Rispens, and G. Vidarsson. 2019. The ligands for human IgG and their effector functions. *Antibodies (Basel)* 8: 30.
2. Montoyo, H. P., C. Vaccaro, M. Hafner, R. J. Ober, W. Mueller, and E. S. Ward. 2009. Conditional deletion of the MHC class I-related receptor FcRn reveals the sites of IgG homeostasis in mice. *Proc. Natl. Acad. Sci. USA* 106: 2788–2793.
3. Ward, E. S., J. Zhou, V. Ghetie, and R. J. Ober. 2003. Evidence to support the cellular mechanism involved in serum IgG homeostasis in humans. *Int. Immunol.* 15: 187–195.
4. Simister, N. E., C. M. Story, H.-L. Chen, and J. S. Hunt. 1996. An IgG-transporting Fc receptor expressed in the syncytiotrophoblast of human placenta. *Eur. J. Immunol.* 26: 1527–1531.
5. Stapleton, N. M., H. K. Einarsdóttir, A. M. Stemerding, and G. Vidarsson. 2015. The multiple facets of FcRn in immunity. *Immunol. Rev.* 268: 253–268.
6. Pyzik, M., K. M. K. Sand, J. J. Hubbard, J. T. Andersen, I. Sandlie, and R. S. Blumberg. 2019. The neonatal Fc receptor (FcRn): a misnomer? *Front. Immunol.* 10: 1540.
7. Dekkers, G., L. Treffers, R. Plomp, A. E. H. Bentlage, M. de Boer, C. A. M. Koeleman, S. N. Lissenberg-Thunnissen, R. Visser, M. Brouwer, J. Y. Mok, et al. 2017. Decoding the human immunoglobulin G-glycan repertoire reveals a spectrum of Fc-receptor- and complement-mediated-effector activities. *Front. Immunol.* 8: 877.
8. Bondt, A., M. Wuhrer, T. M. Kuijper, J. M. Hazes, and R. J. Dolhain. 2016. Fab glycosylation of immunoglobulin G does not associate with improvement of rheumatoid arthritis during pregnancy. *Arthritis Res. Ther.* 18: 274.
9. Hafkenscheid, L., A. Bondt, H. U. Scherer, T. W. Huizinga, M. Wuhrer, R. E. Toes, and Y. Rombouts. 2017. Structural analysis of variable domain glycosylation of anti-citrullinated protein antibodies in rheumatoid arthritis reveals the presence of highly sialylated glycans. *Mol. Cell. Proteomics* 16: 278–287.
10. Koers, J., N. Derksen, W. Falkenburg, P. Ooijevaar-de Heer, M. T. Nurmohamed, G. J. Wolbink, and T. Rispens. 2021. Elevated Fab glycosylation of anti-hinge antibodies. *Scand. J. Rheumatol.* DOI: 10.1002/eji.1830260718.
11. van de Bovenkamp, F. S., N. I. L. Derksen, P. Ooijevaar-de Heer, K. A. van Schie, S. Kruithof, M. A. Berkowska, C. E. van der Schoot, H. IJspeert, M. van der Burg, A. Gils, et al. 2018. Adaptive antibody diversification through *N*-linked glycosylation of the immunoglobulin variable region. *Proc. Natl. Acad. Sci. USA* 115: 1901–1906.
12. Williams, P. J., P. D. Arkwright, P. Rudd, I. G. Scragg, C. J. Edge, M. R. Wormald, and T. W. Rademacher. 1995. Selective placental transport of maternal IgG to the fetus. *Placenta* 16: 749–756.
13. Kibe, T., S. Fujimoto, C. Ishida, H. Togari, Y. Wada, S. Okada, H. Nakagawa, Y. Tsukamoto, and N. Takahashi. 1996. Glycosylation and placental transport of immunoglobulin G. *J. Clin. Biochem. Nutr.* 21: 57–63.
14. Jansen, B. C., A. Bondt, K. R. Reiding, S. A. Scherjon, G. Vidarsson, and M. Wuhrer. 2016. MALDI-TOF-MS reveals differential *N*-linked plasma- and IgG-glycosylation profiles between mothers and their newborns. *Sci. Rep.* 6: 34001.
15. Einarsdottir, H. K., M. H. J. Selman, R. Kapur, S. Scherjon, C. A. M. Koeleman, A. M. Deelder, C. E. Van Der Schoot, G. Vidarsson, and M. Wuhrer. 2013. Comparison of the Fc glycosylation of fetal and maternal immunoglobulin G. *Glycoconj. J.* 30: 147–157.
16. Borghi, S., S. Bournazos, N. K. Thulin, C. Li, A. Gajewski, R. W. Sherwood, S. Zhang, E. Harris, P. Jagannathan, L.-X. Wang, et al. 2020. FcRn, but not FcγRs, drives maternal-fetal transplacental transport of human IgG antibodies. *Proc. Natl. Acad. Sci. USA* 117: 12943–12951.
17. Jennewein, M. F., I. Goldfarb, S. Dolatshahi, C. Cosgrove, F. J. Noelette, M. Krykbaeva, J. Das, A. Sarkar, M. J. Gorman, S. Fischinger, et al. 2019. Fc glycan-mediated regulation of placental antibody transfer. *Cell* 178: 202–215.e14.
18. Jung, S. T., S. T. Reddy, T. H. Kang, M. J. Borrok, I. Sandlie, P. W. Tucker, and G. Georgiou. 2010. Aglycosylated IgG variants expressed in bacteria that selectively bind FcγRI potentiate tumor cell killing by monocyte-dendritic cells. *Proc. Natl. Acad. Sci. USA* 107: 604–609.
19. Lippold, S., S. Nicolardi, E. Domínguez-Vega, A.-K. Heidenreich, G. Vidarsson, D. Reusch, M. Haberger, M. Wuhrer, and D. Falck. 2019. Glycoform-resolved FcγRIIIa affinity chromatography-mass spectrometry. *MAbs* 11: 1191–1196.
20. van de Bovenkamp, F. S., L. Hafkenscheid, T. Rispens, and Y. Rombouts. 2016. The emerging importance of IgG Fab glycosylation in immunity. *J. Immunol.* 196: 1435–1441.
21. Schoch, A., H. Kettenberger, O. Mundigl, G. Winter, J. Engert, J. Heinrich, and T. Emrich. 2015. Charge-mediated influence of the antibody variable domain on FcRn-dependent pharmacokinetics. *Proc. Natl. Acad. Sci. USA* 112: 5997–6002.
22. Datta-Mannan, A., A. Thangaraju, D. Leung, Y. Tang, D. R. Witcher, J. Lu, and V. J. Wroblewski. 2015. Balancing charge in the complementarity-determining regions of humanized mAbs without affecting pI reduces non-specific binding and improves the pharmacokinetics. *MAbs* 7: 483–493.
23. Piche-Nicholas, N. M., L. B. Avery, A. C. King, M. Kavosi, M. Wang, D. M. O'Hara, L. Tchistiakova, and M. Katragadda. 2018. Changes in complementarity-determining regions significantly alter IgG binding to the neonatal Fc receptor (FcRn) and pharmacokinetics. *MAbs* 10: 81–94.
24. Gjølberg, T. T., R. Frick, S. Mester, S. Foss, A. Grevys, L. S. Høydahl, Ø. K. Jørstad, T. Schlothauer, I. Sandlie, M. C. Moe, and J. T. Andersen. 2022. Biophysical differences in IgG1 Fc-based therapeutics relate to their cellular handling, interaction with FcRn and plasma half-life. *Commun. Biol.* 5: 832.
25. Kissel, T., S. Reijm, L. Slot, M. Cavallari, C. Wortel, R. Vergroesen, G. Stoeken-Rijsbergen, J. Kwekkeboom, A. Kampstra, et al. 2020. Antibodies and B cells recognising citrullinated proteins display a broad cross-reactivity towards other post-translational modifications. *Ann. Rheum. Dis.* 79: 472–480.
26. Kissel, T., C. Ge, L. Hafkenscheid, J. C. Kwekkeboom, L. M. Slot, M. Cavallari, Y. He, K. A. van Schie, R. D. Vergroesen, A. S. B. Kampstra, et al. 2022. Surface Ig variable domain glycosylation affects autoantigen binding and acts as threshold for human autoreactive B cell activation. *Sci. Adv.* 8: eabm1759.
27. Guhr, T., J. Bloem, N. I. L. Derksen, M. Wuhrer, A. H. L. Koenderman, R. C. Aalberse, and T. Rispens. 2011. Enrichment of sialylated IgG by lectin fractionation does not enhance the efficacy of immunoglobulin G in a murine model of immune thrombocytopenia. *PLoS One* 6: e21246.
28. Brinkhaus, M., E. J. van der Kooi, A. E. H. Bentlage, P. Ooijevaar-de Heer, N. I. L. Derksen, T. Rispens, and G. Vidarsson. 2022. Human IgE does not bind to human FcRn. *Sci. Rep.* 12: 62.
29. Jansen, B. C., A. Bondt, K. R. Reiding, S. A. Scherjon, G. Vidarsson, and M. Wuhrer. 2016. MALDI-TOF-MS reveals differential *N*-linked plasma- and IgG-glycosylation profiles between mothers and their newborns. *Sci. Rep.* 6: 34001.
30. Jansen, B. C., K. R. Reiding, A. Bondt, A. L. Hipgrave Ederveen, M. Palmblad, D. Falck, and M. Wuhrer. 2015. MassyTools: a high-throughput targeted data processing tool for relative quantitation and quality control developed for glycomic and glycoproteomic MALDI-MS. *J. Proteome Res.* 14: 5088–5098.
31. Schlothauer, T., P. Rueger, J. O. Stracke, H. Hertenberger, F. Fingas, L. Kling, T. Emrich, G. Drabner, S. Seeber, J. Auer, et al. 2013. Analytical FcRn affinity chromatography for functional characterization of monoclonal antibodies. *MAbs* 5: 576–586.
32. Dekkers, G., A. E. H. Bentlage, T. C. Stegmann, H. L. Howie, S. Lissenberg-Thunnissen, J. Zimring, T. Rispens, and G. Vidarsson. 2017. Affinity of human IgG subclasses to mouse Fc gamma receptors. *MAbs* 9: 767–773.
33. Stapleton, N. M., M. Brinkhaus, K. L. Armour, A. E. H. Bentlage, S. W. de Taeye, A. R. Temming, J. Y. Mok, G. Brasser, M. Maas, W. J. E. van Esch, et al. 2019. Reduced FcRn-mediated transcytosis of IgG2 due to a missing glycine in its lower hinge. *Sci. Rep.* 9: 7363.
34. Brinkhaus, M., E. Pannecoucke, E. J. van der Kooi, A. E. H. Bentlage, N. I. L. Derksen, J. Andries, B. Balbino, M. Sips, P. Ulrichts, P. Verheesen, et al. 2022. The Fab region of IgG impairs the internalization pathway of FcRn upon Fc engagement. *Nat. Commun.* 13: 6073.
35. Blumberg, L. J., R. S. Blumberg, S. D. Jones, D. Roopenian, R. G. E. Holgate, T. D. Jones, and A. R. Hearn. 2020. Humanized affinity matured anti-FcRn antibodies. European patent application PCT/US2016/032168, Publication No. EP3294335A4. 2019 Feb 20.
36. Smeele, H. T., E. Röder, H. M. Wintjes, L. J. Kranenburg-van Koppen, J. M. Hazes, and R. J. Dolhain. 2021. Modern treatment approach results in low disease activity in 90% of pregnant rheumatoid arthritis patients: the PreCARA study. *Ann. Rheum. Dis.* 80: 859–864.
37. Kissel, T., K. A. van Schie, L. Hafkenscheid, A. Lundquist, H. Kokkonen, M. Wuhrer, T. W. Huizinga, H. U. Scherer, R. Toes, and S. Rantapää-Dahlqvist. 2019. On the presence of HLA-SE alleles and ACPA-IgG variable domain glycosylation in the phase preceding the development of rheumatoid arthritis. *Ann. Rheum. Dis.* 78: 1616–1620.
38. Jansen, B. C., L. Hafkenscheid, A. Bondt, R. A. Gardner, J. L. Hendel, M. Wuhrer, and D. I. R. Spencer. 2018. HappyTools: a software for high-throughput HPLC data processing and quantitation. *PLoS One* 13: e0200280.
39. Hafkenscheid, L., E. de Moel, I. Smolik, S. Tanner, X. Meng, B. C. Jansen, A. Bondt, M. Wuhrer, T. W. J. Huizinga, R. E. M. Toes, et al. 2019. *N*-linked glycans in the variable domain of IgG anti-citrullinated protein antibodies predict the development of rheumatoid arthritis. *Arthritis Rheumatol.* 71: 1626–1633.
40. Rombouts, Y., A. Willemze, J. J. van Beers, J. Shi, P. F. Kerkman, L. van Toorn, G. M. Janssen, A. Zaldumbide, R. C. Hoeben, G. J. Pruijn, et al. 2016. Extensive glycosylation of ACPA-IgG variable domains modulates binding to citrullinated antigens in rheumatoid arthritis. *Ann. Rheum. Dis.* 75: 578–585.
41. Falck, D., B. C. Jansen, N. de Haan, and M. Wuhrer. 2017. High-throughput analysis of IgG Fc glycopeptides by LC-MS. *Methods Mol. Biol.* 1503: 31–47.
42. Jansen, B. C., D. Falck, N. de Haan, A. L. Hipgrave Ederveen, G. Razdorov, G. Lauc, and M. Wuhrer. 2016. LaCyTools: a targeted liquid chromatography-mass

spectrometry data processing package for relative quantitation of glycopeptides. *J. Proteome Res.* 15: 2198–2210.
43. Bondt, A., Y. Rombouts, M. H. Selman, P. J. Hensbergen, K. R. Reiding, J. M. Hazes, R. J. Dolhain, and M. Wuhrer. 2014. Immunoglobulin G (IgG) Fab glycosylation analysis using a new mass spectrometric high-throughput profiling method reveals pregnancy-associated changes. *Mol. Cell. Proteomics* 13: 3029–3039.
44. Abdiche, Y. N., Y. A. Yeung, J. Chaparro-Riggers, I. Barman, P. Strop, S. M. Chin, A. Pham, G. Bolton, D. McDonough, K. Lindquist, et al. 2015. The neonatal Fc receptor (FcRn) binds independently to both sites of the IgG homodimer with identical affinity. *MAbs* 7: 331–343.
45. Medesan, C., D. Matesoi, C. Radu, V. Ghetie, and E. S. Ward. 1997. Delineation of the amino acid residues involved in transcytosis and catabolism of mouse IgG1. *J. Immunol.* 158: 2211–2217.
46. Stadlmann, J., A. Weber, M. Pabst, H. Anderle, R. Kunert, H. J. Ehrlich, H. Peter Schwarz, and F. Altmann. 2009. A close look at human IgG sialylation and subclass distribution after lectin fractionation. *Proteomics* 9: 4143–4153.
47. Vidarsson, G., G. Dekkers, and T. Rispens. 2014. IgG subclasses and allotypes: from structure to effector functions. *Front. Immunol.* 5: 520.
48. Clements, T., T. F. Rice, G. Vamvakas, S. Barnett, M. Barnes, B. Donaldson, C. E. Jones, B. Kampmann, and B. Holder. 2020. Update on transplacental transfer of IgG subclasses: impact of maternal and fetal factors. *Front. Immunol.* 11: 1920.
49. Moise, K. J., Jr., D. Oepkes, E. Lopriore, and R. G. M. Bredius. 2022. Targeting neonatal Fc receptor: potential clinical applications in pregnancy. *Ultrasound Obstet. Gynecol.* 60: 167–175.
50. Büll, C., R. Nason, L. Sun, J. Van Coillie, D. Madriz Sørensen, S. J. Moons, Z. Yang, S. Arbitman, S. M. Fernandes, S. Furukawa, et al. 2021. Probing the binding specificities of human Siglecs by cell-based glycan arrays. *Proc. Natl. Acad. Sci. USA* 118: e2026102118.
51. Kanda, Y., T. Yamada, K. Mori, A. Okazaki, M. Inoue, K. Kitajima-Miyama, R. Kuni-Kamochi, R. Nakano, K. Yano, S. Kakita, et al. 2007. Comparison of biological activity among nonfucosylated therapeutic IgG1 antibodies with three different *N*-linked Fc oligosaccharides: the high-mannose, hybrid, and complex types. *Glycobiology* 17: 104–118.
52. Jensen, P. F., A. Schoch, V. Larraillet, M. Hilger, T. Schlothauer, T. Emrich, and K. D. Rand. 2017. A two-pronged binding mechanism of IgG to the neonatal fc receptor controls complex stability and igg serum half-life. *Mol. Cell. Proteomics* 16: 451–456.
53. Sela-Culang, I., V. Kunik, and Y. Ofran. 2013. The structural basis of antibody-antigen recognition. *Front. Immunol.* 4: 302.
54. Coloma, M. J., R. K. Trinh, A. R. Martinez, and S. L. Morrison. 1999. Position effects of variable region carbohydrate on the affinity and in vivo behavior of an anti-(1→6) dextran antibody. *J. Immunol.* 162: 2162–2170.
55. Hamza, N., U. Hershberg, C. G. M. Kallenberg, A. Vissink, F. K. L. Spijkervet, H. Bootsma, F. G. M. Kroese, and N. A. Bos. 2015. Ig gene analysis reveals altered selective pressures on Ig-producing cells in parotid glands of primary Sjögren's syndrome patients. *J. Immunol.* 194: 514–521.
56. Lardinois, O. M., L. J. Deterding, J. J. Hess, C. J. Poulton, C. D. Henderson, J. C. Jennette, P. H. Nachman, and R. J. Falk. 2019. Immunoglobulins G from patients with ANCA-associated vasculitis are atypically glycosylated in both the Fc and Fab regions and the relation to disease activity. *PLoS One* 14: e0213215.
57. Zhu, D., H. McCarthy, C. H. Ottensmeier, P. Johnson, T. J. Hamblin, and F. K. Stevenson. 2002. Acquisition of potential N-glycosylation sites in the immunoglobulin variable region by somatic mutation is a distinctive feature of follicular lymphoma. *Blood* 99: 2562–2568.
58. Kinoshita, N., M. Ohno, T. Nishiura, S. Fujii, A. Nishikawa, Y. Kawakami, N. Uozumi, and N. Taniguchi. 1991. Glycosylation at the Fab portion of myeloma immunoglobulin G and increased fucosylated biantennary sugar chains: structural analysis by high-performance liquid chromatography and antibody-lectin enzyme immunoassay using Lens culinaris agglutinin. *Cancer Res.* 51: 5888–5892.
59. Selim, M. A., J. L. Burchette, E. V. Bowers, G. G. de Ridder, L. Mo, S. V. Pizzo, and M. Gonzalez-Gronow. 2011. Changes in oligosaccharide chains of autoantibodies to GRP78 expressed during progression of malignant melanoma stimulate melanoma cell growth and survival. *Melanoma Res.* 21: 323–334.
60. Dashivets, T., M. Thomann, P. Rueger, A. Knaupp, J. Buchner, and T. Schlothauer. 2015. Multi-angle effector function analysis of human monoclonal IgG glycovariants. *PLoS One* 10: e0143520.
61. Bas, M., A. Terrier, E. Jacque, A. Dehenne, V. Pochet-Béghin, C. Beghin, A.-S. Dezetter, G. Dupont, A. Engrand, B. Beaufils, et al. 2019. Fc sialylation prolongs serum half-life of therapeutic antibodies. *J. Immunol.* 202: 1582–1594.
62. Chung, S., V. Nguyen, Y. L. Lin, J. Lafrance-Vanasse, S. J. Scales, K. Lin, R. Deng, K. Williams, G. Sperinde, J. J. Li, et al. 2019. An *in vitro* FcRn-dependent transcytosis assay as a screening tool for predictive assessment of nonspecific clearance of antibody therapeutics in humans. *MAbs* 11: 942–955.
63. Kissel, T., L. Hafkenscheid, T. J. Wesemael, M. Tamai, S. Y. Kawashiri, A. Kawakami, H. S. El-Gabalawy, D. van Schaardenburg, S. Rantapää-Dahlqvist, M. Wuhrer, et al. 2022. IgG anti-citrullinated protein antibody variable domain glycosylation increases before the onset of rheumatoid arthritis and stabilizes thereafter: a cross-sectional study encompassing ~1,500 samples. *Arthritis Rheumatol.* 74: 1147–1158.